# Wavelength tuning of a few-cycle laser pulse by molecular alignment in femtosecond filamentation wake

Jian Wu,[1] Hua Cai,[1] Arnaud Couairon,[2] and Heping Zeng[1,*]
[1]*State Key Laboratory of Precision Spectroscopy, East China Normal University, Shanghai 200062, China*
[2]*Centre de Physique Théorique, CNRS, École Polytechnique, F-91128 Palaiseau, France*
(Received 26 March 2009; published 8 June 2009)

We show by means of numerical simulations that the quantum wake of impulsive molecular alignment provides a simple system to achieve frequency tuning of the broadband spectrum of a few-cycle pulse. A femtosecond pump pulse serves both to form a filament in a molecular gas and to align the molecules. A delayed few-cycle pulse probing the quantum wake is shown to experience a guiding mechanism. Its spectrum is red- or blueshifted while its duration remains comparable to the duration of the incident pulse, resulting in a controllable process to tune the frequency of a few-cycle laser pulse.

DOI: 10.1103/PhysRevA.79.063812 PACS number(s): 42.65.Jx, 52.38.Hb, 33.80.−b, 37.10.Vz

Ultrashort laser pulses containing a few electric field oscillations are required to probe the ultrafast processes in both physics and photochemical reactions, which have enabled numerous applications in extremely nonlinear spectroscopy [1], coherent control [2], and attosecond science in soft x-ray region [3,4]. Few-cycle laser pulses with temporal duration down to sub-10 fs at 800 nm could be emitted directly from oscillators [5,6] in energies of nanojoules. Intense few-cycle laser pulses with micro- or millijoule energies were achieved in solids [7], gas-filled hollow fibers [8], or filaments [9–13] by employing self-phase modulation (SPM) to broaden the spectrum and dispersive elements to recompress the pulse. The central wavelengths of the generated few-cycle pulses were demonstrated to be tunable by means of noncollinear optical parametric amplifications for high pulse energies [14,15] or by self-frequency conversion in photonic-crystal fibers for low energies [16]. By using the time-dependent phase modulation of molecular rotational wave packets in gas-filled hollow fibers [17–19], spectral modulation and compression of ultrashort laser pulses were recently demonstrated, and similar spectral modulation with additional cross-focusing or cross-defocusing effects could also be achieved for near-infrared femtosecond laser pulse in free space [20]. The impulsive molecular alignment with periodic revivals after the extinction of the pump pulse has been extensively studied for molecular-orbital reconstruction [21], high-harmonic generation [22–24], and filamentation [25–31].

In this paper, we numerically show that the central wavelength of a few-cycle laser pulse can be tuned by properly delaying it to the quantum wake of the impulsive molecular alignment achieved by a femtosecond pump pulse which undergoes filamentation in a molecular gas. Filamentation of the pump is governed by a competition between nonlinear effects including Kerr self-focusing, multiphoton absorption, and plasma defocusing, which results in a confinement of the beam diameter of the intense core while its peak intensity may remain clamped over a propagation distance much longer than the Rayleigh range [32]. The pump filament thus allows for manipulation of the molecular orientation over an extended channel which in turn may serve to induce a continuous frequency shift to a few-cycle laser pulse properly delayed in the quantum wake. Similar effects were demonstrated in gas-filled hollow fibers [17–19]. In the filament channel, the quantum wake acts as a guide for the probe pulse over a long distance without the risk of inducing damage as that might encounter in hollow-fiber guiding. Since a filament can be generated remotely in the atmosphere, frequency tuning of ultrashort laser pulses in free space by using the rotational Raman wake of a filament may be used for filament-based remote probing of pollutants and atmospheric applications that require the coverage of specific wavelength domains [32–35]. We not only show how the spectral features can be controlled, but also investigate the spatiotemporal evolution of few-cycle laser pulses with different pulse durations in the quantum wake, for various molecular orientations.

It is well known that when an ultrashort laser pulse propagates in a molecular gas with a rotational period longer than the pulse duration, molecular alignment achieved during the pulse exhibits periodic revivals well after the excitation due to the quantum beatings of the prepopulated rotational states $|JM\rangle$, where $J=0,1,2,\ldots$ and $M=-J,-J+1,\ldots,J-1,J$ account for the orbital momentum and corresponding projection onto the symmetry axis of the molecule, respectively [36]. For an off-resonant excitation, the interaction of a linearly polarized pump pulse with linear molecules can be described by the Hamiltonian $H=H_0-1/4\Delta\alpha E^2\cos^2\theta$, where $H_0=B_0J(J+1)+D_0J^2(J+1)^2$ denotes the field free Hamiltonian, $\theta$ is the angle between the molecular axis and the field polarization of the pulse, $B_0$ and $D_0$ are the rovibrational molecular constants of the molecular gas, $E(t)$ is the amplitude of the pump pulse, and $\Delta\alpha=\alpha_\parallel-\alpha_\perp$ is the polarizability difference between the components parallel and perpendicular to the molecular axis. In our numerical simulations, we characterize the quantum wake by calculating the degree of molecular alignment, featured by the quantity $\langle\langle\cos^2\theta\rangle\rangle$ which is obtained by the following double averaging procedure: the evolution of a rotational state $|\psi\rangle=\Sigma_{JM}C_{JM}|JM\rangle$ during the excitation by the pump pulse is calculated by integrating the Schrödinger equation

*hpzeng@phy.ecnu.edu.cn

 

$i\hbar\,\partial|\psi\rangle/\partial t=H|\psi\rangle$. After extinction of the pump, the population of each rotational state continues to evolve in the field-free Hamiltonian. First the Schrödinger equation is solved for each initial molecular rotational state $|\psi(t=0)\rangle_{J0M0}=|J_0M_0\rangle$, and the degree of molecular alignment at time $t$ is obtained from the population $C_{JM}(t)$ of each rotational state as

$$\langle\cos^2\,\theta(t)\rangle_{J_0M_0}=\sum_{JM}C_{JM}^{*}C_{JM}\langle JM|\cos^2\,\theta|JM\rangle. \tag{1}$$

Then we considered that initial states are populated according to the temperature-dependent Boltzmann distribution. The averaged degree of molecular alignment in the quantum wake is thus obtained by

$$\langle\langle\cos^2\,\theta\rangle\rangle=\frac{\sum_{J_0}P_{J_0}\sum_{M_0=-J_0}^{J_0}\langle\cos^2\,\theta\rangle_{J_0M_0}}{\sum_{J_0}P_{J_0}}, \tag{2}$$

where $P_{J0}$ is the population probability of state $J_0$. For randomly oriented molecules, the average term $\langle\langle\cos^2\,\theta\rangle\rangle$ is equal to 1/3. The molecular orientation tends to be parallel to the field polarization when $\langle\langle\cos^2\,\theta\rangle\rangle$ is greater than 1/3, whereas smaller values indicate an average orientation closer to perpendicular. For reasons explained below, we also calculate the high-order term $\langle\langle\cos^4\,\theta\rangle\rangle$ in a similar way.

We model the propagation of an ultrashort laser pulse in prealigned molecules by including the contributions of the revivals of molecular alignment in the nonlinear envelope equation coupled with an evolution equation for the density $\rho$ of electrons generated by multiphoton ionization [31],

$$\begin{aligned}\frac{\partial E}{\partial z}=&\frac{i}{2k_0}U^{-1}\left(\frac{\partial^2}{\partial r^2}+\frac{1}{r}\frac{\partial}{\partial r}\right)E-i\frac{k_0^{(2)}}{2}\frac{\partial^2E}{\partial t^2}+\frac{k_0^{(3)}}{6}\frac{\partial^3E}{\partial t^3}\\&+U^{-1}\left[T^2ik_0(n_2|E|^2+\delta n)E-\frac{\sigma}{2}(1+i\omega_0\tau_c)\rho E\right.\\&\left.-T\frac{\beta_K}{2}|E|^{2K-2}\left(1-\frac{\rho}{\rho_0}\right)E\right].\end{aligned} \tag{3}$$

In this work, we consider molecular nitrogen at a gas pressure of 1 atm. On the right-hand side of Eq. (3), the successive terms describe diffraction, second- and third-order dispersions, optical Kerr effect with coefficient $n_2=2.3\times10^{-19}$ cm$^2$/W, the change of refraction index $\delta n$ due to molecular alignment which includes the delayed Raman contribution to the nonlinear index, inverse Bremsstrahlung with cross section $\sigma=5.4\times10^{-20}$ cm$^2$ corresponding to the collision time $\tau_c=350$ fs, plasma defocusing, and multiphoton absorption with cross section $\beta_K$, where $K$ denotes the number of photons involved in the multiphoton process. The wave number $k_0$ corresponds to the center wavelength 800 nm of the ultrashort laser pulse, as well as the second- and third-order dispersive coefficients $k_0^{(2)}=0.2$ fs$^2$/cm and $k_0^{(3)}=0.1$ fs$^3$/cm. The operators $U\equiv1+\frac{ik_0^{(1)}}{k_0}\frac{\partial}{\partial t}$ and $T\equiv1+\frac{i}{\omega_0}\frac{\partial}{\partial t}$ account for space-time focusing and self-steepening of the ultrashort laser pulse. The orientation dependent refractive index is given by $\delta n(r,t)=0.5(\rho_0\Delta\alpha/n_0)[\,\langle\langle\cos^2\,\theta(r,t)\rangle\rangle-1/3)+\delta n_{rR}(r,t)]$ [26], where $\rho_0$ is the initial molecular density, $\Delta\alpha=\alpha_{\parallel}-\alpha_{\perp}=1.0$ Å$^3$ and $n_0$ is the linear refractive index. The rotational Raman contribution $\delta n_{rR}$ of the pre-excited molecules is modeled exactly as in Ref. [37] and effectively depends on the pump intensity which is a function of space and time. Thus, both $\delta n_{rR}$ and the degree of molecular alignment $\langle\langle\cos^2\,\theta\rangle\rangle$ depend on space and time. The electron density $\rho$ is calculated by resolving $\partial\rho/\partial t=\sigma_K|E|^{2K}(\rho_0-\rho)$ [32] with orientation-dependent ionization cross section $\sigma_K=\sigma_{K0}[1+(1.5a_2-3.75a_4)(\langle\langle\cos^2\,\theta\rangle\rangle-1/3)+4.375a_4(\langle\langle\cos^4\,\theta\rangle\rangle-1/5)]$ [22] owing to the double-well potential of the diatomic molecules [38], where $a_2=0.39$ and $a_4=-0.21$ and $\sigma_{K0}=6.31\times10^{-140}$ s$^{-1}$ cm$^{22}$/W$^{11}$ (without molecular alignment) [32].

Figure 1 shows the propagation of a 50 fs, 800 nm pump pulse with input power and beam diameter of $P_{\rm in}=2.0P_{\rm cr}$ and 1.5 mm, where $P_{\rm cr}=4.4$ GW is the critical power for self-focusing in nitrogen at 1 atm. The beam is focused by using a lens with the focal length of 30 cm and forms a filament with a beam radius of $\sim50$ $\mu$m over a propagation distance of $\sim38$ cm (from $z=24$ to 62 cm) [Fig. 1(a)] and a clamped peak intensity of $\sim5.0\times10^{13}$ W/cm$^2$ [Fig. 1(b)]. As shown in Fig. 1(c), the pump pulse undergoes an intense spatiotemporal reshaping as identified in [9–11], leading to self-shortening to a full width at half maximum (FWHM) temporal duration of 17 fs at the early stage of the filament. The pulse then propagates with a nearly constant duration until the end of the filament. The evolution of the temporal profile of the pump pulse during the filamentation stage is presented in the inset of Fig. 1(c). The refocused self-shortened pulse is mainly concentrated in the trailing part, on the positive side of the time axis [10,11].

The molecules of diatomic nitrogen are not only partially ionized by optical-field ionization induced by the pump, which participates in regularizing the filament formation, but also spatially aligned through impulsive rotational Raman excitation [36] with periodic revivals after the extinction of the pump pulse. The wake of the filament depends on both the duration and intensity of the pump pulse. Generally, for impulsive rotational Raman excitation, a relatively long pulse duration and high pump intensity will lead to a high degree of molecular alignment. Figure 1(d) shows the calculated molecular alignment signal $\langle\langle\cos^2\,\theta\rangle\rangle$ as a function of time delay after the on-axis peak of the pump pulse for various propagation distances along the filament. The most significant molecular alignment is observed around $z=30$ cm with optimal pulse duration [Fig. 1(c)] and pump intensity [Fig. 1(b)]. Since the pump pulse is strongly reshaped during its propagation, the revivals of molecular alignment indeed strongly depend on the temporal distribution of the propagating pump as well as on its intensity, leading to specific propagation distances to reach optimal parallel or perpendicular orientation. A probe pulse sent after a given delay with respect to the pump will therefore possibly experience a shift in the revivals of molecular alignment [Fig. 1(d)]. As an ultrashort laser pulse propagates collinearly along the pump filament with a delay properly tuned to match the quantum wake of the molecular alignment, it experiences a sturdy frequency shift related to the accumulated nonlinear phase

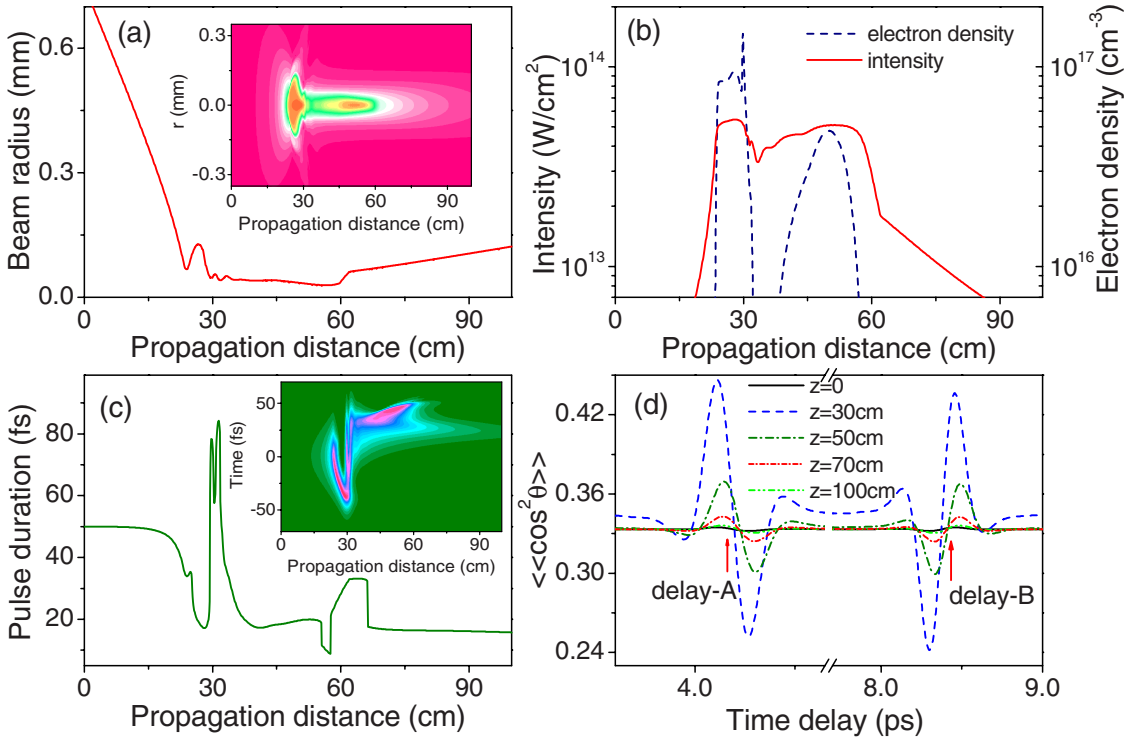


FIG. 1. (Color online) Propagation of a 50 fs, 800 nm pump pulse in molecular nitrogen. (a) Beam radius, (b) peak intensity (solid curve), and on-axis electron density (dashed curve) and (c) on-axis pulse duration versus propagation distance. The insets of (a) and (c) show the evolution of the peak intensity and on-axis temporal profiles, respectively. (d) Molecular alignment signal $\langle\langle \cos^2\theta \rangle\rangle$ calculated on-axis ($r=0$) at various propagation distances.

$\varphi_m$, which reads $\delta\omega(t) = -\partial\varphi_m/\partial t \sim -\partial\delta n(t)/\partial t$. Thus, the probe pulse is expected to experience spectral red- or blue-shift depending on whether its temporal peak is delayed to the rising or falling edge of the molecular alignment revival. Finally, the pump pulse is also strongly reshaped in space, leading to a spatial distribution of the molecular alignment which is included in our simulations and induces additional spatial or spatiotemporal modulation to a temporally delayed probe pulse.

A probe pulse with a temporal duration of 10 fs (~3.75 oscillating cycles) at 800 nm and polarization parallel to the pump is collinearly introduced along the pump filament. A fully self-consistent treatment of the revivals of molecular alignment requires solving the Schrödinger equation over picosecond durations for all propagation steps and for all transverse grid points. In order to make this computational task lighter while still describing the full spatiotemporal coupling of the pump and probe pulses via the quantum wake, the on-axis molecular alignment revival is recalculated at each propagation step, and the transverse intensity profile of the pump pulse that underwent filamentation is used to obtain the spatial distribution of the molecular alignment. The underlying assumption is that of a molecular alignment signal proportional to the excitation intensity for pump intensities smaller than $1.0\times10^{14}$ W/cm$^2$ [26,39]. The lifetime of the plasma generated by multiphoton ionization induced by the pump filament is much longer than the delay between pump and probe. The plasma decay time lasts typically several tens of picoseconds. The plasma density in the wake of the pump filament is therefore taken as the initial electron density experienced by the probe pulse sent after the pump with a relative temporal delay of several picoseconds. The input power and beam diameter of the few-cycle probe pulse are, respectively, set to be $P_{in}=0.5P_{cr}$ and 4.0 mm, which is collimated with respect to the pump. In the absence of the advancing pump pulse which forms the filament and achieves molecular alignment, the few-cycle probe pulse propagates quasilinearly: it undergoes negligible spatial diffraction and only slight temporal broadening due to group-velocity dispersion. As will be seen below, the probe pulse sent in the quantum wake may become sufficiently intense to be also potentially affected by self-induced effects mixed with those of the revivals. However, our choice of parameters guarantees that the probe intensity remains below the ionization threshold. Since the probe pulse duration is much shorter than the time delay of the molecular alignment response to a pulse excitation (~several tens of femtoseconds) [27], it modifies molecular alignment at later delays but experiences only the molecular alignment induced by the pump; this enhances self-focusing only in the very core of the probe overlapping with the original filament.

As shown in Fig. 2, the propagation dynamics of the probe pulse is significantly influenced by the pump filament when its temporal peak is properly tuned to match the quantum wake of the molecular alignment. During the falling edge of the molecular alignment around the half-revival time [delay-A as shown in Fig. 1(d)], the spectrum of the probe pulse is first gradually blueshifted before the beginning of the pump filament [Fig. 2(a)]. This is due to a cross-phase modulation effect mediated by the revivals of molecular

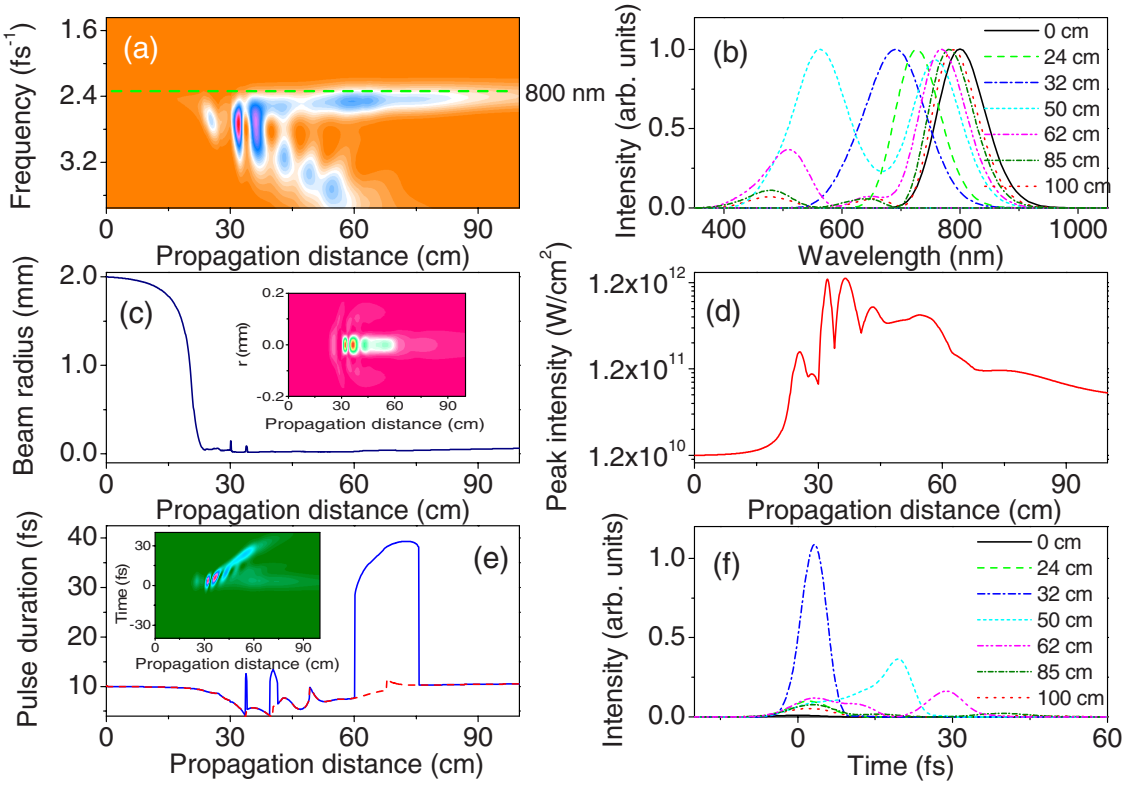


FIG. 2. (Color online) Propagation of a 10 fs probe pulse in the quantum wake when its temporal peak is tuned to the molecular alignment revival at delay-A as shown in Fig. 1(d). (a) Evolution of the on-axis spectral profile, (c) beam radius, (d) peak intensity, and (e) on-axis pulse duration of the probe pulse (solid curve: whole pulse; dashed curve: most intense subpulse) versus propagation distance. The evolution of the spatial and on-axis temporal profiles of the probe pulse are shown in the insets of (c) and (e), respectively. (b) Spectral (normalized), and (f) temporal profiles of the probe pulse at various propagation distances.

alignment. The spectrum is then considerably broadened during the early stage of the pump filament and split into two spectral components due to both intense self-phase modulation and cross-phase modulation mediated by the quantum wake of molecular alignment. During this stage, the peak intensity of the probe increases and eventually evolves into a stable intense light channel accompanying the quantum wake of the pump pulse. Figure 2(b) plots the detailed spectral profiles of the probe pulse at various propagation distances. It clearly suggests that a continuously blueshifted spectrum with a 100 nm maximum shift of the central wavelength is readily achievable for the few-cycle probe pulse before the occurrence of spectral splitting. As shown in Figs. 2(c) and 2(d), the beam radius of the probe pulse decreases while its peak intensity increases before stabilizing to form a stable light channel with an almost constant beam radius of $\sim 25$ $\mu$m and peak intensity of $\sim 5.0 \times 10^{11}$ W/cm$^2$. These values are smaller than the typical values obtained for a long pulse filament of $\sim 50$ $\mu$m and $\sim 10^{13}$ W/cm$^2$ [32], though the peak intensity is close to the nonionizing intense light channel reported a few years ago [40]. Here, the guiding mechanism proceeds differently since it is mainly the quantum wake that guides the probe and makes it propagate in the form of an intense light channel. The fast decrease in the full width at half maximum of the initially collimated probe beam does not correspond to a whole beam collapse but is mainly due to the increased degree of molecular alignment in the narrow portion of the probe overlapping with the original pump filament of width of $\sim 50$ $\mu$m. The probe pulse sees an increased refractive index which not only includes the contribution of the revival but also that of the self-induced instantaneous Kerr effect acting against plasma defocusing (proportional to $-0.5\rho/\rho_c$, where $\rho_c$ is the critical plasma density [32]). For example at delay-A, by adding the molecular alignment and plasma contributions, the average increase in the refractive index on the propagation axis experienced by the temporal peak of the probe is calculated to be $4.0 \times 10^{-6}$. This results in an overall guiding of the probe pulse. After the end of the pump filament, the beam radius of the probe pulse gradually increases to $\sim 60$ $\mu$m while its peak intensity decreases to $\sim 6.5 \times 10^{10}$ W/cm$^2$ over the simulated propagation distance of 1.0 m. The detailed spatial evolution of the probe pulse is plotted in the inset of Fig. 2(c), which clearly indicates guiding of the probe pulse by the quantum wake.

The spectral evolution of the temporally delayed probe pulse can be further understood by simultaneously looking at the evolution of its temporal profile along the propagation axis. As shown in Fig. 2(f) and the inset of Fig. 2(e), the probe pulse is first gradually delayed to the positive side of the time axis in keeping with the induced spectral blueshift and normal dispersion of the molecular gas. Pulse splitting occurs owing to the intense phase modulation of the probe pulse, and the temporally delayed pulse peak with noticeably

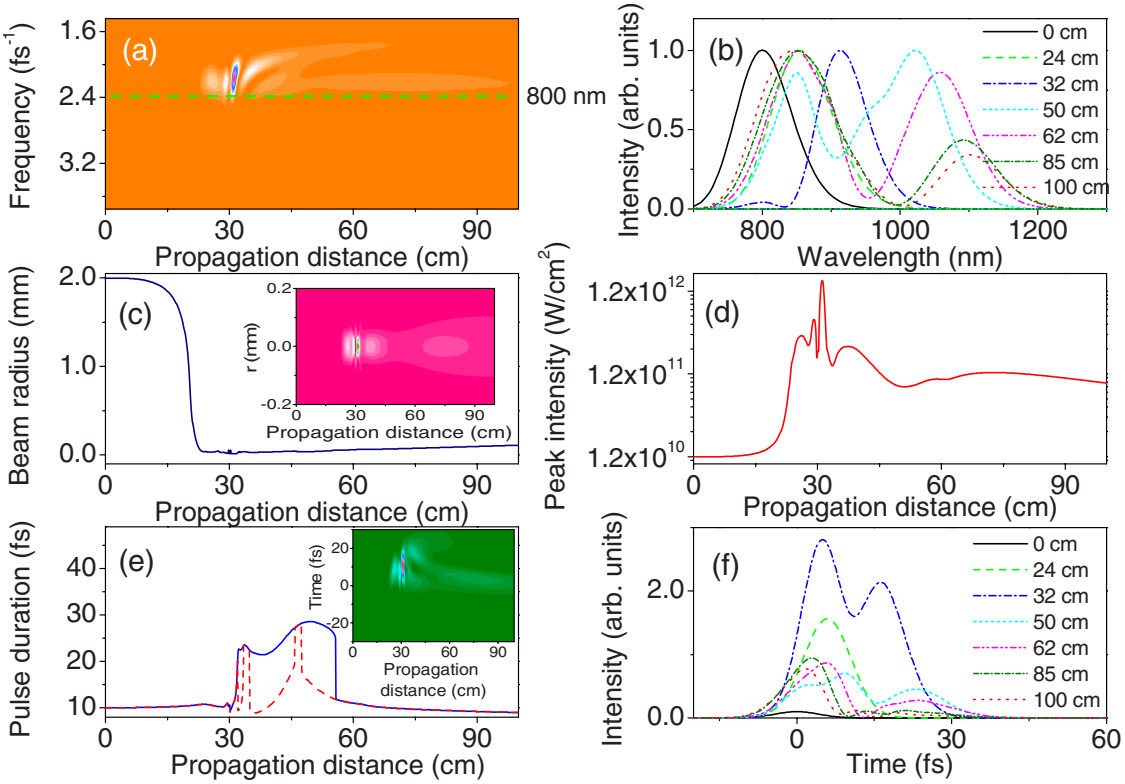


FIG. 3. (Color online) Same presentation as in Fig. 2 but for the probe pulse matching the molecular alignment revival at delay-B as shown in Fig. 1(d).

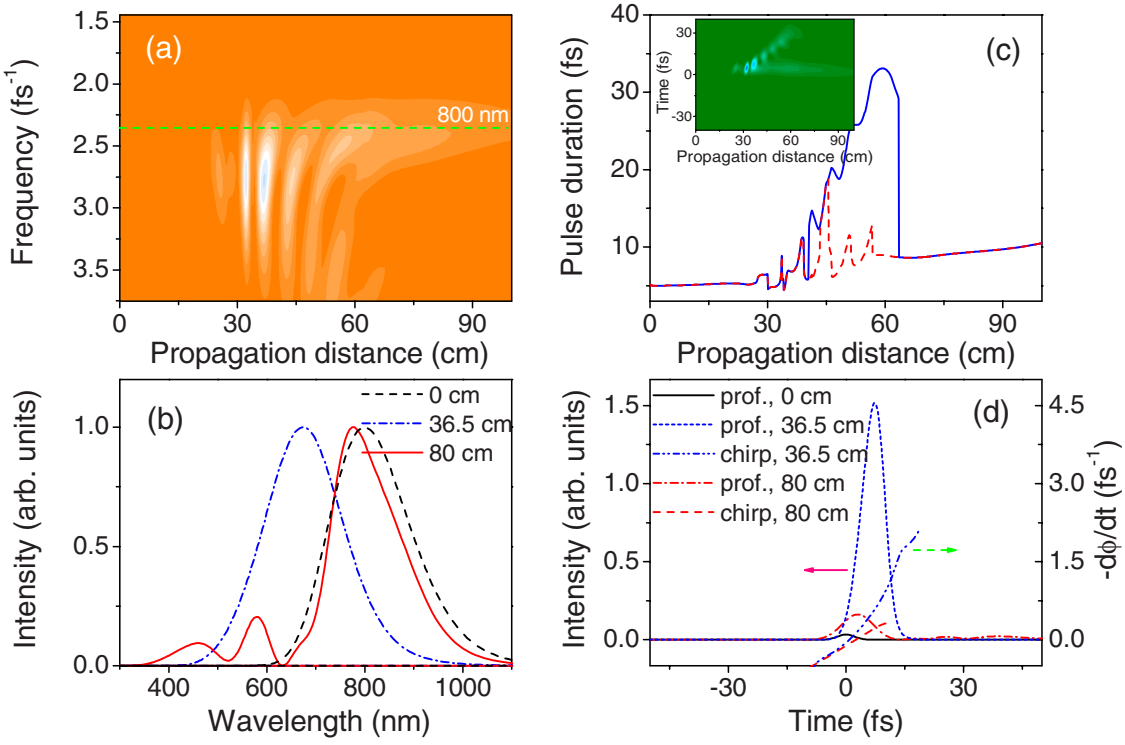


FIG. 4. (Color online) Propagation of a 5 fs probe pulse in the quantum wake when its temporal peak is tuned to the molecular alignment revival at delay-A as shown in Fig. 1(d). (a) Evolution of the on-axis spectral profile and (c) on-axis pulse duration of the probe pulse versus propagation distance. The inset of (c) shows the evolution of the on-axis temporal profile of the probe pulse. (b) On-axis spectral profiles of the probe pulse (normalized) at various propagation distances. (d) Corresponding temporal profiles (solid curves) and frequency chirps (dashed curves), defined as the time derivative of the phase (instantaneous frequency).

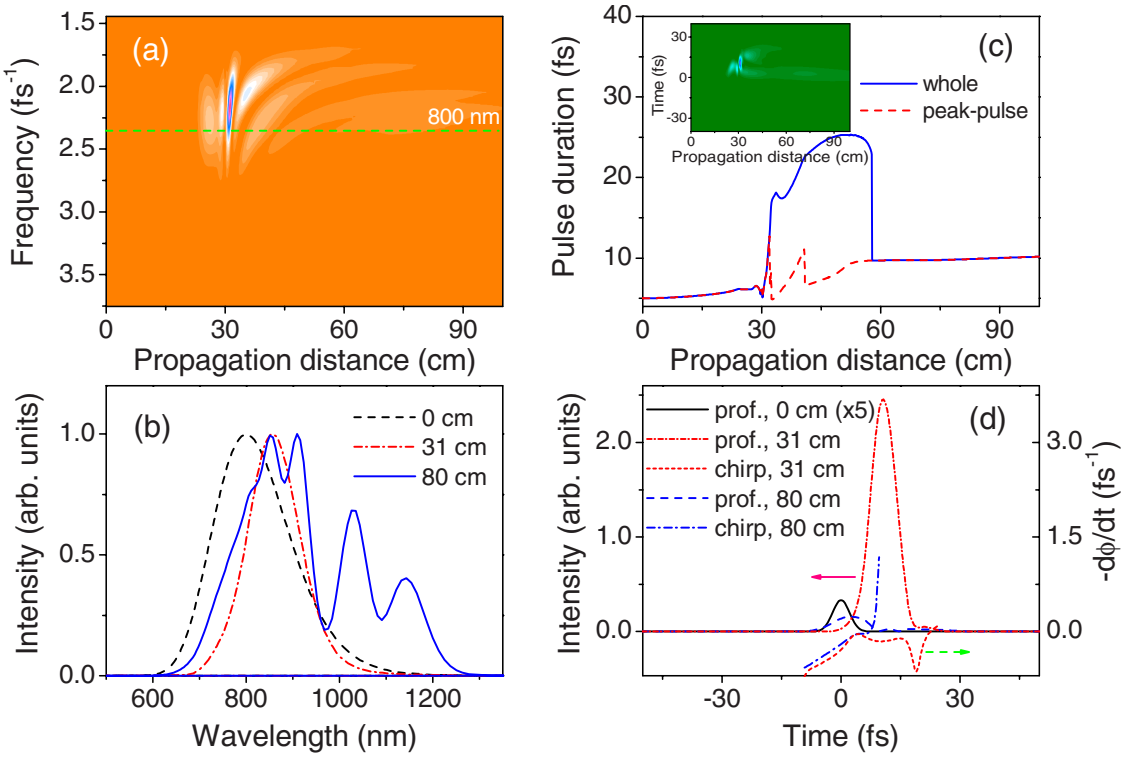


FIG. 5. (Color online) Same presentation as in Fig. 4 but for the probe pulse matching the molecular alignment revival at delay-B as shown in Fig. 1(d).

blueshifted frequency components is eventually dispersed and leads to a single pulse peak as shown in Fig. 2(a) [32]. The evolution of the pulse duration along the propagation of the probe pulse is shown in Fig. 2(e) During the guiding stage, the duration of the probe pulse fluctuates around the input value of 10 fs and compression down to sub-5 fs durations could be obtained at specific distances. The sudden increase in the pulse duration form $z=60$ to 75 cm is directly due to the temporal splitting of the probe pulse into a double-peak structure as shown in the inset of Fig. 2(e). The duration of the most intense subpulse is monitored independently and is found to remain shorter than 10 fs, as shown in Fig. 2(e) (dashed curve).

We interpret the spatiotemporal evolution of the temporally delayed probe pulse as dominated by cross-phase modulation mediated by the molecular alignment in the wake of the pump filament. From this analysis, we could obtain few-cycle laser pulses with desired frequency shift and pulse duration at specific propagation distances. Alternatively, it is possible to generate these frequency shifted few-cycle pulses at a given propagation distance by using a pump beam that forms a filament starting from the desired length to the target [41,42] and by tuning the temporal peak of the probe pulse to various revival times of the molecular alignment so as to control the cross-phase modulation effect it undergoes. Figure 3 shows an example of the spatiotemporal evolution of the probe pulse as its temporal peak is tuned to delay-B, i.e., to the rising edge of the molecular alignment revival as shown in Fig. 1(d). In contrast with delay-A, the spectrum of the few-cycle probe pulse is noticeably redshifted for delay-B [Figs. 3(a) and 3(b)], but similarly to delay-A, the probe pulse forms a guided light channel with a well-confined beam radius [Fig. 3(c)] and a peak intensity that remains intense over an extended distance [Fig. 3(d)]. As we can see from Fig. 3(e), the duration of the probe pulse also fluctuates around the incident value of 10 fs; the sudden increase in the pulse duration from $z=32$ to 56 cm is due to the occurrence of temporal splitting [see inset of Fig. 3(e)] which makes the evolution of the FWHM duration discontinuous since the two separating pulses are characterized by a single duration. The corresponding temporal profiles of the probe pulse at various propagation distances for delay-B are shown in Fig. 3(f).

Propagation dynamics of the few-cycle probe pulse are also studied for different delays during the revivals of molecular alignment in the wake of the pump filament, which lead to the observation of different spatiotemporal dynamics. Typically, for revivals of molecular alignment with $\langle\langle\cos^2\theta\rangle\rangle < 1/3$, the probe pulse also undergoes a significant frequency shift but eventually evolves into a doughnut-shaped hollow beam. This is due to the cross-defocusing effect mediated by the molecules oriented perpendicularly to the polarization of the probe, thus leading to a decrease in the experienced refractive index [30]. Simulations are also performed for even shorter probe pulses. For example for ultrashort laser pulse with a duration of 5 fs ($\sim$1.87 oscillating cycles) at 800 nm, a similar guiding dynamics is observed with the expected spectral blueshift [Figs. 4(a) and 4(b)] or redshift [Figs. 5(a) and 5(b)] when the peak of the probe pulse is tuned to match the falling (delay-A) or rising (delay-B) edges of the revival of molecular alignment in the wake of the pump filament. The relative spectral broadening

is less significant than for the case of 10 fs probe pulse, which we interpret as due to the fact that the shortest pulses experience a more uniform cross-phase modulation along the time axis. For instance, at delay-A, the averaged spectral width (FWHM) of the probe pulse broadens and becomes 1.92 and 1.16 times the input spectral width of the 10 and 5 fs probe pulses, respectively. When the temporal peak of the probe pulse is tuned to match the molecular alignment revival at delay-B, these spectral broadening factors become 1.47 and 1.06 for the 10 and 5 fs input probe pulses, respectively. Meanwhile, as shown in Figs. 4(c) and 4(d) and Figs. 5(c) and 5(d), the pulse duration increases to ~10 fs, the associated frequency chirp [dashed curves in Figs. 4(d) and 5(d)] is due to dispersion from the molecular gas. We check numerically that the pulses can be further compressed to durations close to or in certain cases shorter than the input duration of 5 fs by using suitable dispersion compensator, such as chirped mirrors and prism pairs modeled through their second- and third-order dispersions, to compensate at least partially for the linear dispersions of the molecular gas.

In summary, we have shown numerically that the wavelength of a few-cycle probe pulse can be readily red- or blueshifted by properly tuning its delay so as to match the revival of molecular alignment in the quantum wake of a femtosecond pump pulse undergoing filamentation. The duration of the frequency shifted probe pulse remains comparable with the initial duration. This method provides us an alternative approach to tune the frequency of few-cycle laser pulse for various applications, such as remote atmospheric probing.

This work was funded in part by National Natural Science Fund (Grants No. 10525416 and No. 10804032), National Key Project for Basic Research (Grant No. 2006CB806005), Projects from Shanghai Science and Technology Commission (Grant No. 08ZR1407100), Program for Changjiang Scholars and Innovative Research Team in University, and Shanghai Educational Development Foundation (Grant No. 2008CG29).

[1] T. Brabec and F. Krausz, Rev. Mod. Phys. **72**, 545 (2000).
[2] B. Kohler, V. V. Yakovlev, J. Che, J. L. Krause, M. Messina, K. R. Wilson, N. Schwentner, R. M. Whitnell, and Y. J. Yan, Phys. Rev. Lett. **74**, 3360 (1995).
[3] M. Drescher, M. Hentschel, R. Kienberger, G. Tempea, C. Spielmann, G. Reider, P. Corkum, and F. Krausz, Science **291**, 1923 (2001).
[4] I. J. Sola, E. Mével, L. Elouga, E. Constant, V. Strelkov, L. Poletto, P. Villoresi, E. Benedetti, J.-P. Caumes, S. Stagira, C. Vozzi, G. Sansone, and M. Nisoli, Nat. Phys. **2**, 319 (2006).
[5] J. Zhou, G. Taft, C. Huang, M. M. Murnane, H. C. Kapteyn, and I. P. Christov, Opt. Lett. **19**, 1149 (1994).
[6] R. Ell, U. Morgner, F. X. Kärtner, J. G. Fujimoto, E. P. Ippen, V. Scheuer, M. Tilsch, T. Tschudi, M. J. Lederer, A. Boiko, and B. Luther-Davies, Opt. Lett. **26**, 373 (2001).
[7] A. Baltuska, Z. Wei, M. S. Pshenichnikov, and D. A. Wiersma, Opt. Lett. **22**, 102 (1997).
[8] M. Nisoli, S. Stagira, S. D. Silvestri, O. Svelto, S. Sartania, Z. Cheng, M. Lenzner, C. Spielmann, and F. Krausz, Appl. Phys. B: Lasers Opt. **65**, 189 (1997).
[9] C. P. Hauri, W. Kornelis, F. W. Helbing, A. Heinrich, A. Couairon, A. Mysyrowicz, J. Biegert, and U. Keller, Appl. Phys. B: Lasers Opt. **79**, 673 (2004).
[10] A. Couairon, J. Biegert, C. P. Hauri, W. Kornelis, F. W. Helbing, U. Keller, and A. Mysyrowicz, J. Mod. Opt. **53**, 75 (2006).
[11] S. Akturk, A. Couairon, M. Franco, and A. Mysyrowicz, Opt. Express **16**, 17626 (2008).
[12] F. Théberge, N. Aközbek, W. Liu, A. Becker, and S. L. Chin, Phys. Rev. Lett. **97**, 023904 (2006).
[13] A. Zaïr, A. Guandalini, F. Schapper, M. Holler, J. Biegert, L. Gallmann, A. Couairon, M. Franco, A. Mysyrowicz, and U. Keller, Opt. Express **15**, 5394 (2007).
[14] G. Cerullo, M. Nisoli, S. Stagira, S. De Silvestri, G. Tempea, F. Krausz, and K. Ferencz, Opt. Lett. **24**, 1529 (1999).
[15] A. Shirakawa, I. Sakane, M. Takasaka, and T. Kobayashi, Appl. Phys. Lett. **74**, 2268 (1999).
[16] N. Ishii, C. Y. Teisset, S. Kohler, E. E. Serebryannikov, T. Fuji, T. Metzger, F. Krausz, A. Baltuška, and A. M. Zheltikov, Phys. Rev. E **74**, 036617 (2006).
[17] R. A. Bartels, T. C. Weinacht, N. Wagner, M. Baertschy, C. H. Greene, M. M. Murnane, and H. C. Kapteyn, Phys. Rev. Lett. **88**, 013903 (2001).
[18] N. Zhavoronkov and G. Korn, Phys. Rev. Lett. **88**, 203901 (2002).
[19] F. Zhong, H. Jiang, and Q. Gong, Opt. Express **17**, 1472 (2009).
[20] H. Cai, J. Wu, A. Couairon, and H. Zeng, Opt. Lett. **34**, 827 (2009).
[21] J. Itatani, J. Levesque, D. Zeidler, H. Niikura, H. Pépin, J. Kieffer, P. Corkum, and D. Villeneuve, Nature (London) **432**, 867 (2004).
[22] T. Kanai, S. Minemoto, and H. Sakai, Nature (London) **435**, 470 (2005).
[23] G. H. Lee, I. J. Kim, S. B. Park, T. K. Kim, and C. H. Nam, Opt. Lett. **33**, 2083 (2008).
[24] J. Wu, H. Qi, and H. Zeng, Phys. Rev. A **77**, 053412 (2008).
[25] F. Calegari, C. Vozzi, S. Gasilov, E. Benedetti, G. Sansone, M. Nisoli, S. De Silvestri, and S. Stagira, Phys. Rev. Lett. **100**, 123006 (2008).
[26] J. Wu, H. Cai, H. Zeng, and A. Couairon, Opt. Lett. **33**, 2593 (2008).
[27] S. Varma, Y.-H. Chen, and H. M. Milchberg, Phys. Rev. Lett. **101**, 205001 (2008).
[28] Y. Chen, C. Marceau, F. Théberge, M. Châteauneuf, J. Dubois, and S. L. Chin, Opt. Lett. **33**, 2731 (2008).
[29] A. C. Bernstein, M. McCormick, G. M. Dyer, J. C. Sanders, and T. Ditmire, Phys. Rev. Lett. **102**, 123902 (2009).
[30] H. Cai, J. Wu, Y. Peng, and H. Zeng, Opt. Express **17**, 5822 (2009).

[31] J. Wu, H. Cai, Y. Peng, and H. Zeng, Phys. Rev. A **79**, 041404(R) (2009).
[32] A. Couairon and A. Mysyrowicz, Phys. Rep. **441**, 47 (2007).
[33] J. Yu, D. Mondelain, G. Ange, R. Volk, S. Niedermeier, J. P. Wolf, J. Kasparian, and R. Sauerbrey, Opt. Lett. **26**, 533 (2001).
[34] K. Stelmaszczyk, P. Rohwetter, G. Méjean, J. Yu, E. Salmon, J. Kasparian, R. Ackermann, J. Wolf, and L. Wöste, Appl. Phys. Lett. **85**, 3977 (2004).
[35] J.-F. Daigle, G. Méjean, W. Liu, F. Théberge, H. L. Xu, Y. Kamali, J. Bernhardt, A. Azarm, Q. Sun, P. Mathieu, G. Roy, J.-R. Simard, and S. L. Chin, Appl. Phys. B: Lasers Opt. **87**, 749 (2007).
[36] H. Stapelfeldt and T. Seideman, Rev. Mod. Phys. **75**, 543 (2003).
[37] E. Nibbering, G. Grillon, M. Franco, B. Prade, and A. Mysyrowicz, J. Opt. Soc. Am. B **14**, 650 (1997).
[38] J. Wu, H. Zeng, and C. Guo, Phys. Rev. A **74**, 065403 (2006); **75**, 043402 (2007).
[39] R. Boyd, *Nonlinear Optics*, 2nd ed. (Academic Press, New York, 2003).
[40] G. Méchain, A. Couairon, Y.-B. André, C. D'Amico, M. Franco, B. Prade, S. Tzortzakis, A. Mysyrowicz, and R. Sauerbrey, Appl. Phys. B: Lasers Opt. **79**, 379 (2004).
[41] A. Couairon, Appl. Phys. B: Lasers Opt. **76**, 789 (2003).
[42] G. Fibich, Y. Sivan, Y. Ehrlich, E. Louzon, M. Fraenkel, S. Eisenmann, Y. Katzir, and A. Zigler, Opt. Express **14**, 4946 (2006).